



Cite this: *Org. Biomol. Chem.*, 2017, **15**, 9996

Received 23rd October 2017,  
Accepted 20th November 2017

DOI: 10.1039/c7ob02605f

rsc.li/obc

## Automated glycan assembly of galactosylated xyloglucan oligosaccharides and their recognition by plant cell wall glycan-directed antibodies†

Pietro Dallabernardina,<sup>a,b</sup> Colin Ruprecht,<sup>a</sup> Peter J. Smith,<sup>c</sup> Michael G. Hahn,<sup>id c</sup> Breeanna R. Urbanowicz<sup>id c</sup> and Fabian Pfrengle<sup>id \*a,b</sup>

We report the automated glycan assembly of oligosaccharides related to the plant cell wall hemicellulosic polysaccharide xyloglucan. The synthesis of galactosylated xyloglucan oligosaccharides was enabled by introducing *p*-methoxybenzyl (PMB) as a temporary protecting group for automated glycan assembly. The generated oligosaccharides were printed as microarrays, and the binding of a collection of xyloglucan-directed monoclonal antibodies (mAbs) to the oligosaccharides was assessed. We also demonstrated that the printed glycans can be further enzymatically modified while appended to the microarray surface by *Arabidopsis thaliana* xyloglucan xylosyltransferase 2 (*AtXXT2*).

Xyloglucan (XG) is the most abundant hemicellulosic polysaccharide in the primary cell walls of higher plants.<sup>1</sup> By hydrogen bonding to cellulose microfibrils, a cellulose-XG network is formed that provides the cell wall with both strength and flexibility.<sup>2,3</sup> Xyloglucans are composed of a  $\beta$ -(1,4)-D-glucan backbone decorated with  $\alpha$ -D-xylopyranosyl (*Xylp*) residues at O-6, which are often further extended by addition of galactosyl and fucosyl substituents. To date, 24 different naturally occurring xyloglucan side-chain structures have been identified.<sup>4</sup> Despite this diversity, galactose substitution at O-2 of one or more of the xylose residues is present in all plant species, suggesting that this modification plays an important structural or functional role in the plant cell wall.<sup>5,6</sup>

Distinct glycan epitopes in structurally different XGs can be localized in plant cell walls by performing fluorescent microscopy of plant material after staining with cell wall glycan-directed monoclonal antibodies.<sup>7</sup> Many antibodies are

available that recognize different molecular structures in XGs.<sup>8–10</sup> However, the limited information that is available on their epitope specificity prevents a comprehensive interpretation of the differential binding patterns obtained with XG-directed antibodies. To determine the precise epitopes bound by these antibodies, well-defined oligosaccharides are required that can either be obtained by purification from plants<sup>11</sup> or by chemical synthesis. Unlike the preparation by enzymatic hydrolysis of natural XG, chemical synthesis can provide XG oligosaccharides whose diversity is not limited by the specificities of hydrolytic enzymes.

Despite their importance as tools for plant cell wall biology, only a few examples of syntheses of XG oligosaccharides have been reported. The only chemical solution-phase synthesis of XG oligosaccharides beyond tetrasaccharides was reported by Sakai *et al.*, and in this case a XG nonasaccharide was assembled based on a block coupling approach using glycosylimidate donors.<sup>12</sup> Libraries of larger XG oligosaccharides have been prepared by chemo-enzymatic synthesis using glycosynthase enzymes.<sup>13</sup> However, the diversity of accessible products was limited by the substrate specificity of the glycosynthases and the availability of oligosaccharide starting materials obtained by enzymatic digestion of XG polymers.

We recently reported the synthesis of xyloglucan oligosaccharides<sup>15</sup> using automated glycan assembly,<sup>16</sup> a powerful technology for the synthesis of plant cell wall oligosaccharides.<sup>17–21</sup> The oligosaccharides were printed as microarrays<sup>22</sup> and the epitopes for several antibodies recognizing XG were partially determined.<sup>23</sup> However, our original collection did not contain galactosylated oligosaccharides; therefore, no galactose-specific antibodies could be identified. Herein, we report the automated glycan assembly of a new glycan collection, including the synthesis of two galactosylated XG oligosaccharides and their use in a microarray-based assay to investigate the epitopes for a number of additional XG-directed antibodies.

We selected building blocks (BBs) 1–4 for automated glycan assembly of the XG oligosaccharides (Fig. 1). While the selection of BBs 1 and 4 as typical monosaccharide BBs was

<sup>a</sup>Department of Biomolecular Systems, Max Planck Institute of Colloids and Interfaces, Am Mühlenberg 1, 14476 Potsdam, Germany.

E-mail: Fabian.Pfrengle@mpikg.mpg.de

<sup>b</sup>Freie Universität Berlin, Institute of Chemistry and Biochemistry, Arnimallee 22, 14195 Berlin, Germany

<sup>c</sup>Complex Carbohydrate Research Center, University of Georgia, 315 Riverbend Road, Athens, GA 30602, USA

† Electronic supplementary information (ESI) available: Experimental procedures for solution- and automated solid-phase reactions and characterization data for all compounds. See DOI: 10.1039/c7ob02605f



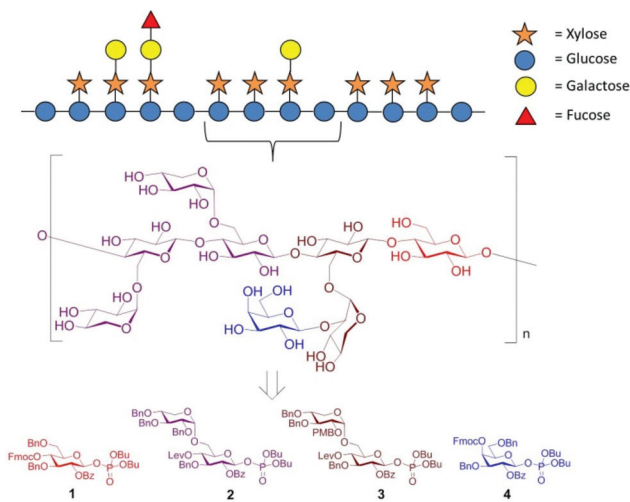
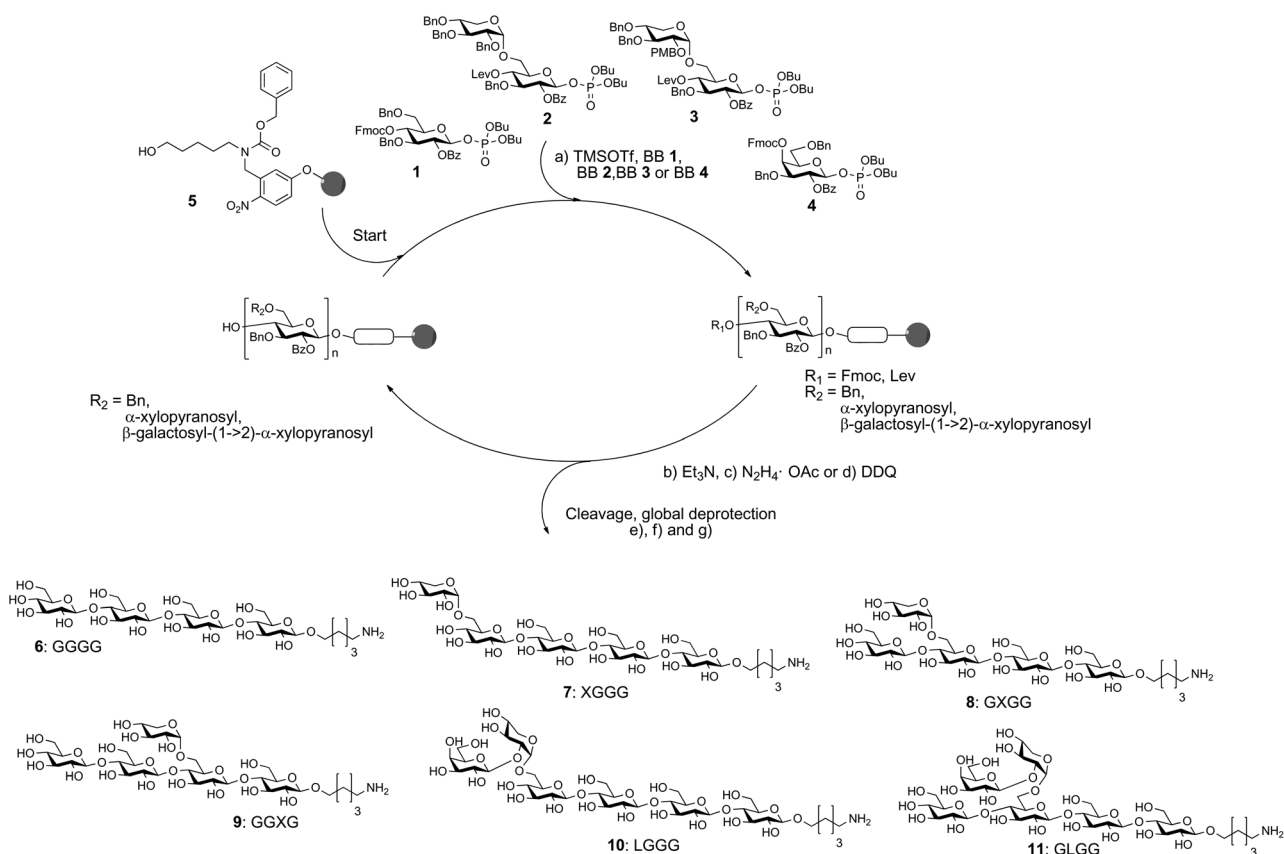


**Fig. 1** Schematic representation of the hemicellulosic polysaccharide xyloglucan and the monosaccharide building blocks required for the automated assembly of representative oligosaccharide fragments.

straightforward, we decided to introduce the xylosyl residues using disaccharide BBs 2 and 3. Our previous work has shown that it is advantageous to avoid difficulties in the stereo-selective formation of  $\alpha$ -xylosidic linkages by using disaccharide BBs where this challenging linkage has been preinstalled. Both disaccharide BBs were equipped with a temporary levulinoyl protecting group for chain elongation. In BB 3, an additional temporary protecting group was installed at the C2-position of the xylopyranose to enable attachment of an additional galactose residue. We chose *p*-methoxybenzyl (PMB)<sup>24</sup> as a non-participating protecting group, as opposed to 2-naphthylmethyl (NAP), which was previously used in automated glycan assembly of xylan oligosaccharides,<sup>20</sup> since we had observed the occasional loss of primary benzyl groups during oxidative cleavage of NAP ethers. To ensure  $\beta$ -selectivity in the glycosylation reactions, all BBs were equipped with benzoyl esters (Bz) in the C2-position. Dibutyl phosphate was used as the leaving group for all BBs because they resulted in improved conversion compared with the corresponding



**Scheme 1** Automated glycan assembly of XG oligosaccharides 6–11. Reagents and conditions: (a) 1 or 2  $\times$  3.7 equiv. BB 1, TMSOTf, CH<sub>2</sub>Cl<sub>2</sub>, –30 °C (5 min)  $\rightarrow$  –15 °C (30 min) or 2  $\times$  3.7 equiv. BB 2, TMSOTf, CH<sub>2</sub>Cl<sub>2</sub>, –35 °C (5 min)  $\rightarrow$  –15 °C (35 min); 2  $\times$  3.7 equiv. BB 3, TMSOTf, CH<sub>2</sub>Cl<sub>2</sub>, –35 °C (5 min)  $\rightarrow$  –10 °C (35 min) or 2  $\times$  3.7 equiv. BB 4, TMSOTf, CH<sub>2</sub>Cl<sub>2</sub>, –35 °C (5 min)  $\rightarrow$  –20 °C (40 min) (Module A); (b) 3 cycles of 20% NEt<sub>3</sub> in DMF, 25 °C (5 min) (Module B); (c) N<sub>2</sub>H<sub>4</sub>·OAc (155 mM) in pyridine/AcOH/H<sub>2</sub>O 4 : 1 : 0.25, 25 °C (30 min) (Module C); (d) 1 cycle DDQ (0.1 M) in DCE/MeOH/H<sub>2</sub>O 64 : 16 : 1, 40 °C (20 min) (Module D); (e) CH<sub>2</sub>Cl<sub>2</sub>, *hν* (305 nm); (f) NaOMe, THF/MeOH, 12 h; (g) H<sub>2</sub>, Pd/C, EtOAc/MeOH/H<sub>2</sub>O/HOAc, 12 h. **6:** 14%; **7:** 10%; **8:** 36%; **9:** 42%; **10:** 13%; **11:** 8% (yields are based on resin loading). The letter code below the structures refers to a common nomenclature of XG oligosaccharides.<sup>14</sup>



thioglycoside donors (see ESI†). BBs 1–4 were synthesized as previously reported or in analogy (see ESI†).<sup>15,19</sup>

The automated glycan assembly of cellulose and XG oligosaccharides 6–9 was performed by iterative addition of BBs 1 and 2 to linker-functionalized resin 5,<sup>25</sup> UV-induced cleavage of the photo-labile linker, and subsequent global deprotection to remove all remaining benzoyl ester and benzyl ether protecting groups (Scheme 1). To obtain galactosylated XG oligosaccharide 10, the oligosaccharide backbone was assembled using BBs 1 and 3, followed by oxidative cleavage of the PMB group, then glycosylation of the resulting free hydroxyl with galactose BB 4. For removal of the PMB group, a single incubation cycle with 0.1 M DDQ was sufficient, while six cycles of DDQ treatment are normally required to remove NAP groups on the solid phase.<sup>20</sup> During the glycosylation reaction with BB 3, we observed small amounts of side products that resulted from the loss of the PMB group under the acidic glycosylation conditions followed by glycosylation of the free hydroxyl with additional equivalents of disaccharide BB 3. Consequently, further experiments suggested that the formation of these side products can be suppressed using lower glycosylation temperatures.

For assembly of XG oligosaccharide 11, two different reaction sequences are conceivable: (i) the galactose is attached to the fully assembled oligosaccharide backbone or (ii) the PMB group is cleaved immediately after glycosylation with disaccharide BB 3 and the resulting free hydroxyl at the xylose residue is galactosylated with BB 4 followed by Lev cleavage and final glucosylation with BB 1. Initially, we tested the second approach but did not observe any conversion to the desired compound. This might result from steric hindrance by the galactose, preventing further extension of the backbone. Fortunately, when the full oligosaccharide backbone was assembled first, we were able to obtain the desired XG oligosaccharide 11 in satisfactory overall yield.

We printed the newly synthesized compounds, together with the previously prepared XG oligosaccharides, on microarray slides and probed the binding specificities of 23 xyloglucan-directed mAbs. Using this approach we identified nine mAbs that bind to galactosylated XG oligosaccharides (Fig. 2). Strong binding of most of these antibodies suggests that a single galactosyl residue  $\beta$ -1,2-linked to xylose is sufficient for these antibodies to bind. While the galactosyl moiety was essential for these mAbs to bind, we were able to further characterize mAb CCRC-M87, which also displays weak binding to several XG oligosaccharides that lack galactose substitution (Fig. 2).

Although it was previously shown that the 23 mAbs evaluated in this study bind non-fucosylated natural xyloglucan polymers in ELISA experiments,<sup>10</sup> many of the mAbs did not recognize any of the printed XG oligosaccharides (ESI Fig. 1†). In contrast to natural XG polysaccharides in which the galactose substituents are located at defined xylose residues of a highly xylosylated glucan backbone, the synthetic glycans contained only single side chains; therefore, we hypothesized that more complex substitution patterns might be required for

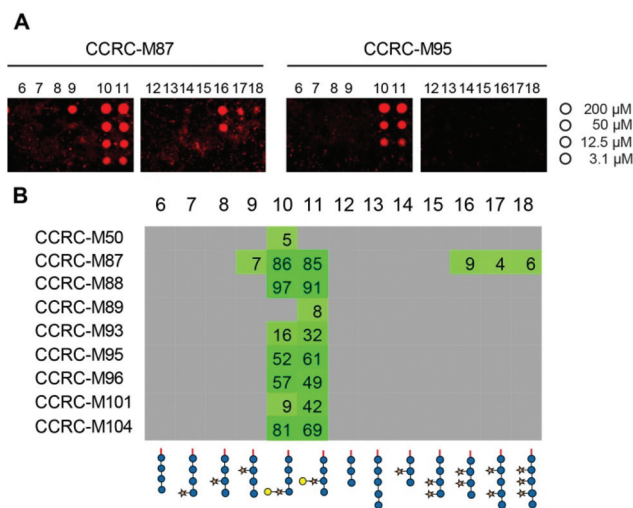


Fig. 2 Plant cell wall directed monoclonal antibodies (mAbs) bind to xyloglucan fragments 6–18. (A) Microarray scans showing binding of selected antibodies to xyloglucan oligosaccharides. Each compound was printed in four concentrations as indicated on the right. (B) Binding of mAbs specific to galactosylated xyloglucan. The obtained fluorescence values were normalized against the highest value on the microarray and are displayed as percentages. To remove background signals, only values above 4% are displayed. The complete list of investigated xyloglucan-directed mAbs can be found in ESI Fig. 1.†

recognition for a subset of the mAbs. To enzymatically attach additional xylosyl residues to the chemically synthesized XG oligosaccharides, we incubated the glycan microarray with *Arabidopsis thaliana* xyloglucan xylosyltransferase 2 (*AtXXT2*) and UDP-xylose.<sup>26,27</sup> *AtXXT2* is an  $\alpha$ -1,6-D-xylosyltransferase that transfers a xylosyl residue from UDP-xylose to the glucan backbone of XG.

Expression of the soluble catalytic domain of *AtXXT2* was achieved by transient transfection of suspension culture HEK293 cells using a strategy similar to prior studies on glycosyltransferases involved in hemicellulosic polysaccharide biosynthesis.<sup>28,29</sup> Incubation of the glycan array with *AtXXT2* resulted in strong mAb-binding to the linear tetra- and pentaglycosides (compounds 6 and 13, Fig. 3), indicating successful transfer of a xylosyl residue to these compounds. Triglycoside 12 was too short to be utilized as a substrate by *AtXXT2*, based on the observation that no (CCRC-M86) or only very weak (CCRC-M100) fluorescent signals were observed after the *AtXXT2* reaction. Unfortunately, we did not identify additional antibodies that recognize the galactosylated XG oligosaccharides (ESI Fig. 1†). This is likely because either the enzymatic transfer of xylose to compounds 10 and 11 was too inefficient (detected with CCRC-M100, Fig. 3), or the remaining mAbs recognize epitopes that have not been generated.

In conclusion, we have prepared six cellulose and XG oligosaccharides with and without galactose substitution using automated glycan assembly. The syntheses were enabled by using PMB for the first time as a non-participating protecting group in solid-phase oligosaccharide synthesis. The procured





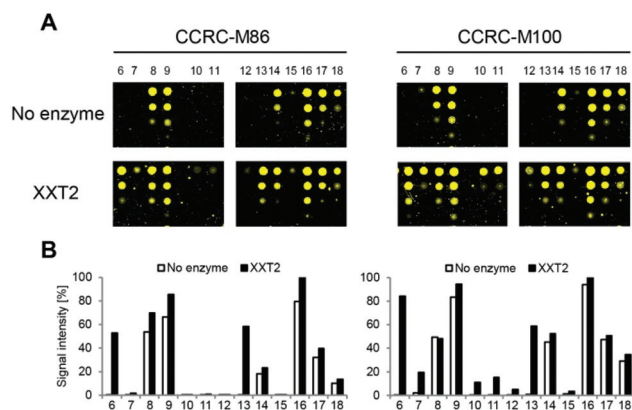


**Fig. 3** Glycosyltransferase assays using xyloglucan oligosaccharides 6–18 on a glycan microarray. (A) The activity of xyloglucan xylosyltransferase 2 (XXT2) was assessed after incubation of the glycans appended to the microarray chip with purified AtXXT2 and UDP-xylose. Enzymatically modified glycans were detected with CCRC-M86 or CCRC-M100. (B) Quantification of fluorescent signals for each of the compounds with before and after XXT2-catalyzed xylosyl addition. Averages of the four printed concentrations are displayed.

compounds have been printed, together with previously synthesized XG oligosaccharides, as microarrays and screened against 23 anti-xyloglucan mAbs. We were able to partially characterize the binding specificities for a number of mAbs that recognize galactosylated XG structures. Furthermore, we successfully used a xyloglucan xylosyltransferase, AtXXT2, to enzymatically add additional xylosyl residues to the printed XG oligosaccharides. When used in combination with cell wall-directed antibodies, our glycan microarray platform has thus great potential for characterizing glycosyltransferases of unknown function.

## Conflicts of interest

There are no conflicts to declare.

## Acknowledgements

We gratefully acknowledge financial support from the Max Planck Society, the Fonds der Chemischen Industrie (Liebig Fellowship to F. P.), and the German Research Foundation (DFG, Emmy Noether program PF850/1-1 to F. P.). We thank Max Bartetzko for providing galactose building block 4. Generation of the CCRC series of monoclonal antibodies used in this work was supported by grants from the United States Natural Science Foundation Plant Genome Program (DBI-0421683 and IOS-0923992). P. J. S. and B. R. U. were supported by the BioEnergy Science Center (DE-PS02-06ER64304), a US Department of Energy Bioenergy Research Center supported by the Office of Biological and Environmental Research in the U.S. Department of Energy Office of Science. P. J. S. and B. R. U. also thank the Center for Plant and Microbial

Complex Carbohydrates (DEFG0296ER20097) for equipment support. Open Access funding is provided by the Max Planck Society.

## References

- 1 A. Ebringerova, Z. Hromadkova and T. Heinze, *Adv. Polym. Sci.*, 2005, **186**, 1–67.
- 2 M. McCann, B. Wells and K. Roberts, *J. Cell Sci.*, 1990, **96**, 323–324.
- 3 C. Somerville, S. Bauer, G. Brininstool, M. Facette, T. Hamann, J. Milne, E. Osborne, A. Paredez, S. Persson, T. Raab, S. Vorwerk and H. Youngs, *Science*, 2004, **306**, 2206–2211.
- 4 M. Pauly and K. Keegstra, *Annu. Rev. Plant Biol.*, 2016, **67**, 235–259.
- 5 A. Schultink, L. Liu, L. Zhu and M. Pauly, *Plants*, 2014, **3**, 526–542.
- 6 Y. Kong, M. J. Peña, L. Renna, U. Avci, S. Pattathil, S. T. Tuomivaara, X. Li, W.-D. Reiter, F. Brandizzi, M. G. Hahn, A. G. Darvill, W. S. York and M. A. O'Neill, *Plant Physiol.*, 2015, **167**, 1296–1306.
- 7 J. P. Knox, *Curr. Opin. Plant Biol.*, 2008, **11**, 308–313.
- 8 S. E. Marcus, Y. Verhertbruggen, C. Hervé, J. J. Ordaz-Ortiz, V. Farkas, H. L. Pedersen, W. G. T. Willats and J. P. Knox, *BMC Plant Biol.*, 2008, **8**, 60–71.
- 9 H. L. Pedersen, J. U. Fangel, B. McCleary, C. Ruzanski, M. G. Rydahl, M. C. Ralet, V. Farkas, L. v. Schantz, S. E. Marcus, M. C. F. Andersen, R. Field, M. Ohlin, J. P. Knox, M. H. Clausen and W. G. T. Willats, *J. Biol. Chem.*, 2012, **287**, 39429–39438.
- 10 S. Pattathil, U. Avci, D. Baldwin, A. G. Swennes, J. A. McGill, Z. Popper, T. Bootten, A. Albert, R. H. Davis, C. Chennareddy, R. Dong, B. O'Shea, R. Rossi, C. Leoff, G. Freshour, R. Narra, M. O'Neil, W. S. York and M. G. Hahn, *Plant Physiol.*, 2010, **153**, 514–525.
- 11 S. T. Tuomivaara, K. Yaoi, M. A. O'Neill and W. S. York, *Carbohydr. Res.*, 2015, **402**, 56–66.
- 12 K. Sakai, Y. Nakahara and T. Ogawa, *Tetrahedron Lett.*, 1990, **31**, 3035–3038.
- 13 R. Fauré, M. Saura-Valls, H. Brumer, A. Planas, S. Cottaz and H. Driguez, *J. Org. Chem.*, 2006, **71**, 5151–5161.
- 14 S. C. Fry, W. S. York, P. Albersheim, A. Darvill, T. Hayashi, J.-P. Joseleau, Y. Kato, E. P. Lorences, G. A. Maclachlan, M. McNeil, A. J. Mort, J. S. G. Reid, H. U. Seitz, R. R. Selvendran, A. G. J. Voragen and A. R. White, *Physiol. Plant.*, 1993, **89**, 1–3.
- 15 P. Dallabernardina, F. Schumacher, P. H. Seeberger and F. Pfrengle, *Org. Biomol. Chem.*, 2016, **14**, 309–313.
- 16 P. H. Seeberger, *Acc. Chem. Res.*, 2015, **48**, 1450–1463.
- 17 D. Schmidt, F. Schumacher, A. Geissner, P. H. Seeberger and F. Pfrengle, *Chem. – Eur. J.*, 2015, **21**, 5709–5713.
- 18 M. P. Bartetzko, F. Schumacher, H. S. Hahn, P. H. Seeberger and F. Pfrengle, *Org. Lett.*, 2015, **17**, 4344–4347.



- 19 M. P. Bartzko, F. Schumacher, P. H. Seeberger and F. Pfrenge, *J. Org. Chem.*, 2017, **82**, 1842–1850.
- 20 D. Senf, C. Ruprecht, G. H. M. de Kruijff, S. O. Simonetti, F. Schumacher, P. H. Seeberger and F. Pfrenge, *Chem. – Eur. J.*, 2017, **23**, 3197–3205.
- 21 P. Dallabernardina, F. Schumacher, P. H. Seeberger and F. Pfrenge, *Chem. – Eur. J.*, 2017, **23**, 3191–3196.
- 22 C. D. Rillahan and J. C. Paulson, *Annu. Rev. Biochem.*, 2011, **80**, 797–823.
- 23 C. Ruprecht, M. P. Bartzko, D. Senf, P. Dallabernardina, I. Boos, M. C. F. Andersen, T. Kotake, J. P. Knox, M. G. Hahn, M. H. Clausen and F. Pfrenge, *Plant Physiol.*, 2017, **175**, 1094–1104.
- 24 H. Takaku and K. Kamaike, *Chem. Lett.*, 1982, **11**, 189–192.
- 25 S. Eller, M. Collot, J. Yin, H. S. Hahm and P. H. Seeberger, *Angew. Chem., Int. Ed.*, 2013, **52**, 5858–5861.
- 26 A. Faik, N. J. Price, N. V. Raikhel and K. Keegstra, *Proc. Natl. Acad. Sci. U. S. A.*, 2002, **99**, 7797–7802.
- 27 D. M. Cavalier and K. Keegstra, *J. Biol. Chem.*, 2006, **281**, 34197–34207.
- 28 B. R. Urbanowicz, M. J. Peña, H. A. Moniz, K. W. Moremen and W. S. York, *Plant J.*, 2014, **80**, 197–206.
- 29 B. R. Urbanowicz, V. S. Bharadwaj, M. Alahuhta, M. J. Peña, V. V. Lunin, Y. J. Bomble, S. Wang, J.-Y. Yang, S. T. Tuomivaara, M. E. Himmel, K. W. Moremen, W. S. York and M. F. Crowley, *Plant J.*, 2017, **91**, 931–949.

